

## High-resolution photoemission study of Peierls instability in thallium chains on copper(100)

This article has been downloaded from IOPscience. Please scroll down to see the full text article.

1991 J. Phys.: Condens. Matter 3 5425

(<http://iopscience.iop.org/0953-8984/3/28/017>)

View [the table of contents for this issue](#), or go to the [journal homepage](#) for more

Download details:

IP Address: 171.66.16.147

The article was downloaded on 11/05/2010 at 12:22

Please note that [terms and conditions apply](#).

## High-resolution photoemission study of Peierls instability in thallium chains on copper(100)

C Binns and C Norris

Department of Physics and Astronomy, University of Leicester, Leicester LE3 0JP, UK

Received 11 January 1991, in final form 19 April 1991

**Abstract.** The  $E$ - $k$  dispersion of the  $6p$  derived valence band of Tl chains adsorbed on Cu(100) has been measured as a function of density and temperature using high-resolution angle-resolved photoelectron spectroscopy. The most dense chain structure, at a coverage of  $\theta = 0.67$  undergoes a Peierls distortion with a corresponding band gap at the Fermi level, estimated to be 0.25 eV. At temperatures below about 225 K, LEED shows two-dimensional order with an alignment of the distortion between neighbouring chains. The measured dispersion at room temperature indicates that the overlayer still retains a distorted chain structure and the observed loss of overlayer spots in the LEED pattern is due to the loss of inter-chain registry. At the lower coverage,  $\theta = 0.6$ , a less dense chain structure occurs which shows no evidence for a Peierls distortion. The suppression of any superstructure is ascribed to the greater commensurability between the overlayer and the substrate.

### 1. Introduction

One-dimensional (1D) systems have been the focus of much interest because of their unique behaviour and the fact that, for them, certain classes of problems are exactly soluble (Lieb and Mattis 1966, Sölyom 1979). According to Peierls (1964) an atomic chain with a partially filled conduction band can lower its energy by undergoing a periodic lattice distortion which opens a gap in the electron energy spectrum at the Fermi level. In consequence a 1D jellium metal is inherently unstable against the formation of a charge density wave (CDW). For a quasi-1D system in a real solid the CDW can be commensurate or incommensurate with the underlying lattice. Excitations in the superlattice consist of phase changes in the distortion and maybe of the phason (in the case of incommensurate CDWs) or soliton (in the case of nearly commensurate CDWs) type (Schultz 1979).

Many examples of quasi-1D systems have been studied including organic charge transfer salts, polymers and transition metal complexes. Atomic chains adsorbed on oriented surfaces in ultra-high vacuum represent a further example which is more controllable. The interaction with the substrate, however, results in an interfacial energy term which for a high degree of commensurability between overlayer and substrate lattices is capable of suppressing 1D behaviour (Binns *et al* 1986). Earlier studies demonstrated the existence of a Peierls distortion in Tl chains adsorbed along the  $\langle 110 \rangle$  furrows of a Cu(100) surface (Binns *et al* 1984).

We present here a high-resolution angle-resolved photoelectron spectroscopy study of this system as a function of density and temperature in the range where 1D chains

form. By using low-energy ( $h\nu \leq 10$  eV) photons we have been able to map the Tl 6p electron bands with an energy and momentum resolution of 105 meV and  $0.04 \text{ \AA}^{-1}$ , sufficient to show the formation of the Peierls gap. From consideration of the Fermi level crossing of the band we suggest the most dense chain structure contains more Tl atoms than was earlier proposed.

## 2. Experimental details

The measurements were made in a  $\mu$ -metal screened ultra-high vacuum chamber equipped with a 4-grid LEED display optics and a VSW HA50 angle-resolving electron energy analyser mounted on a two circle goniometer. Thallium was evaporated from a Knudsen cell source onto a Cu(100) single crystal held at room temperature. The substrate was prepared by repeated cycles of argon ion sputtering and annealing. The base pressure in the chamber was  $2 \times 10^{-10}$  mbar and was never higher than  $5 \times 10^{-10}$  mbar during deposition.

UV radiation from a hydrogen discharge lamp was dispersed by a 1 m normal-incidence monochromator and focused through a LiF window onto the sample at an incident angle of  $45^\circ$ . The monochromator resolution at 7.87 eV photon energy was 50 meV. The electron energy analyser was operated in a fixed analyser transmission (FAT) mode with a pass energy of 10 eV giving a nominal energy resolution of 100 meV. The combined energy resolution measured from the width of the Fermi edge was 105 meV.

The angle resolution was  $4^\circ$  as estimated from the size of the light spot and the entrance aperture of the HA50 input lens. For electrons emitted at 3 eV and  $45^\circ$  to the normal the uncertainty in  $k$ ,  $\Delta k$ , is thus  $0.04 \text{ \AA}^{-1}$  or about 4% of the Brillouin zone width. Such a high resolution is a consequence of the low photon energy used.

## 3. Results

### 3.1. Growth

Previous studies of the Tl/Cu(100) system have shown that thallium grows in the Stranski-Krastanov mode on Cu(100) forming a dense hexagonal monolayer with further deposits nucleating as islands on top of this layer (Binns *et al* 1984, Binns and Norris 1982). At sub-monolayer coverages and room temperature, LEED indicates the formation of a  $\begin{pmatrix} 2 & 2 \\ 2 & 2 \end{pmatrix}$  arrangement initially which then disappears over a small range of coverage. No further structures are observed until close to the monolayer when a  $\begin{pmatrix} 4 & 0 \\ 2 & 2 \end{pmatrix}$  pattern, ascribed to a distorted hexagonal structure appears. Continued deposition results in a  $\begin{pmatrix} 4 & 0 \\ 2 & 6 \end{pmatrix}$  phase which is a dense hexagonal monolayer with a nearest neighbour distance close to the metallic Tl diameter ( $3.46 \text{ \AA}$ ). The  $\begin{pmatrix} 2 & 2 \\ 2 & 2 \end{pmatrix}$  arrangement observed at room temperature was ascribed to a regular array of Tl dimers (Binns *et al* 1984).

A sub-monolayer kink observed in the Auger-signal versus time (AS- $t$ ) plot has been associated with the transition from quasi-1D structures to 2D overlayers (Binns *et al* 1984). In the coverage range between the disappearance of the room temperature  $\begin{pmatrix} 2 & 2 \\ 2 & 2 \end{pmatrix}$  structure and the sub-monolayer kink, cooling the sample to 100 K produces a set of new and complex LEED patterns each existing over a narrow coverage range. We believe this is due to Tl forming linear chains which ascend a 'devils staircase' of commensurability

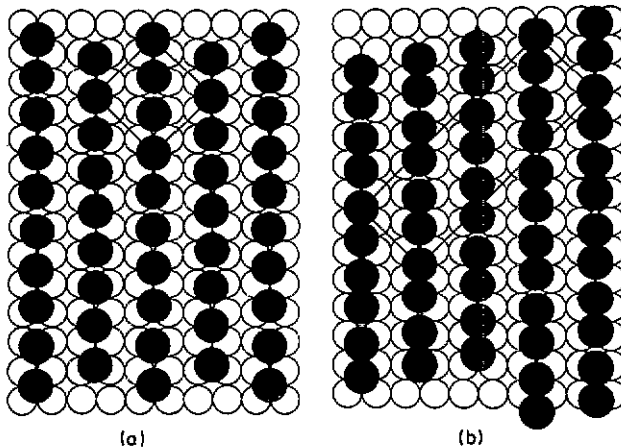


Figure 1. Proposed Tl chain structures on Cu(100) at low temperature. (a)  $(\begin{smallmatrix} 2 \\ 2 \end{smallmatrix})$  structure at a coverage,  $\theta = 0.6$ . (b)  $(\begin{smallmatrix} 6 \\ 6 \end{smallmatrix})$  structure at a coverage,  $\theta = 0.67$ .

between the overlayer and substrate lattice. The most reproducible structures in this range have a  $(\begin{smallmatrix} 2 \\ 2 \end{smallmatrix})$  unit mesh which we associate with an undistorted linear chain as shown in figure 1(a) and a  $(\begin{smallmatrix} 6 \\ 2 \end{smallmatrix})$  unit mesh which, based on evidence to be presented later, is ascribed to the structure in figure 1(b), that is, a more dense linear chain which has undergone a Peierls distortion. Warming either of these structures to 300 K causes the overlayer LEED patterns to disappear. In an earlier report (Binns *et al* 1984) it was suggested that the  $(\begin{smallmatrix} 6 \\ 2 \end{smallmatrix})$  pattern was due to a Peierls distorted chain of lower density. Careful measurements now confirm that it occurs after the low-temperature  $(\begin{smallmatrix} 2 \\ 2 \end{smallmatrix})$  structure and is closer to the sub-monolayer AS- $t$  break.

In the following the coverage  $\theta$  is defined as the atom number density relative to the dense hexagonal structure at the monolayer coverage in which the metallic Tl diameter of 3.46 Å is assumed ( $\theta = 1$ ). According to our model the most dense linear chain arrangement at the sub-monolayer break in the AS- $t$  curve (figure 1(b) has a coverage  $\theta = 0.67$ . Elsewhere, the coverage is assumed to vary linearly with deposition time. The  $(\begin{smallmatrix} 2 \\ 2 \end{smallmatrix})$  structure shown in figure 1(a) thus corresponds to  $\theta = 0.6$ .

Figure 2 shows a sequence of normal emission photoelectron spectra for different Tl coverages obtained with a photon energy of 7.87 eV and with the sample at 100 K. The most notable change is the appearance of extra features at  $-0.28$  eV,  $-0.89$  eV and  $-2.68$  eV, over the narrow coverage range  $0.55 < \theta < 0.63$ . These are most intense at the coverage  $\theta = 0.6$  corresponding to the brightest  $(\begin{smallmatrix} 2 \\ 2 \end{smallmatrix})$  LEED pattern at low temperature. They are attributed to umklapp features from the copper states scattered into the normal direction by the ordered overlayer (figure 1(a)). Increasing the photon energy to 9.71 eV causes them to disappear. This would not occur in the case of direct emission from the electron states of an overlayer which was not extended normal to the surface.

At very low coverages increased emission at the Fermi level, shown in the inset of figure 2 is attributed to a Tl 6p state resonating with the substrate continuum.

### 3.2. Tl 6p valence band dispersion

Figure 3 shows angle-resolved photoelectron spectra obtained with the  $(\begin{smallmatrix} 2 \\ 2 \end{smallmatrix})$  Tl overlayer at a coverage  $\theta = 0.6$  and a temperature of 100 K. The Tl 6p feature from any ordered

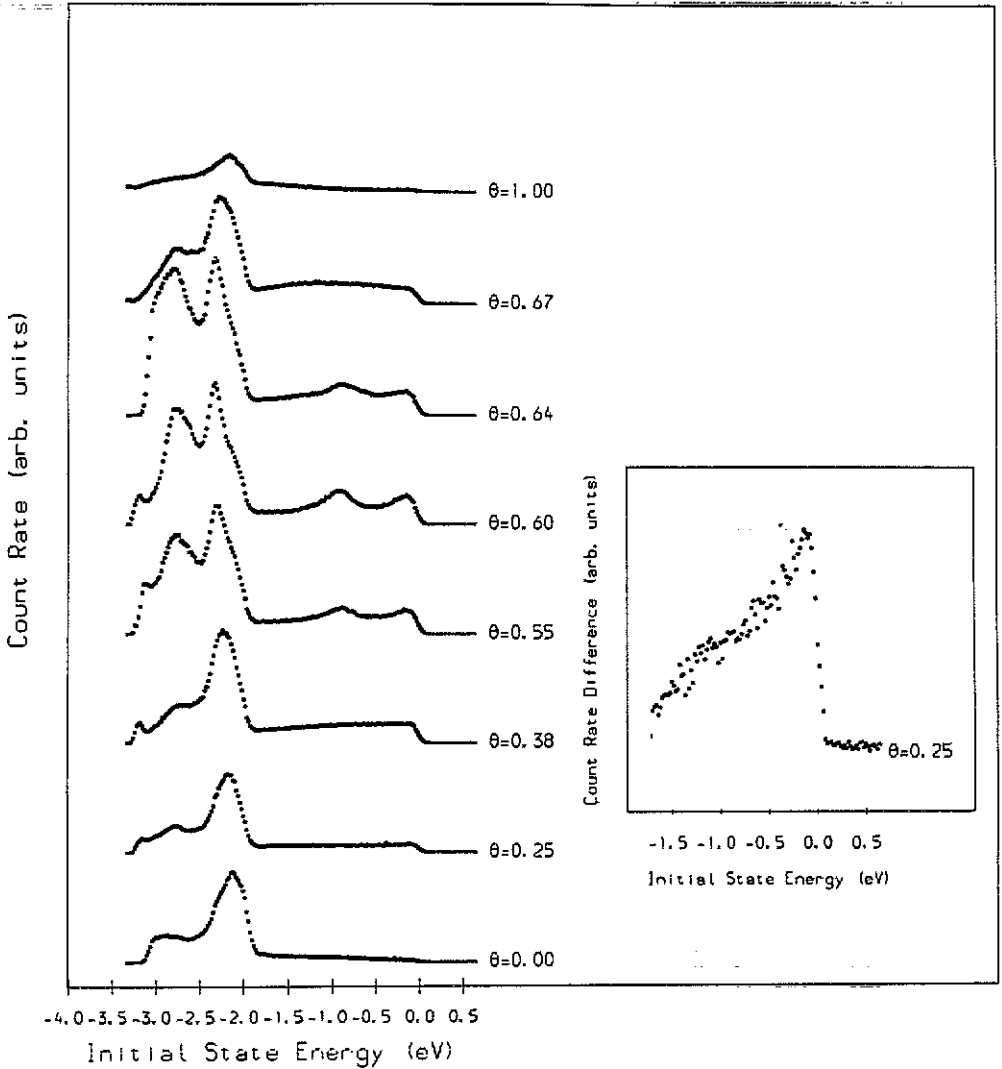


Figure 2. Normal emission photoelectron spectra at  $h\nu = 7.87$  eV, taken with the sample at 100 K, as a function of TI coverage,  $\theta$ .

overlayer will not be observed at normal emission since it is from an unfilled band in the second zone. At emission angles,  $\theta_c \geq 40^\circ$ , a feature appears at the Fermi level and disperses to lower energy (figure 3) with increasing angle. There are no significant features from the substrate in this region and we ascribe the peak to direct emission from the thallium 6p band in the reduced zone scheme, that is, electrons undergoing an umklapp from the second zone. The 6p band dispersion derived from the data in figure 3 is plotted in figure 4. This plot includes data points from photoemission spectra taken at the slightly lower coverage,  $\theta = 0.55$ , at which the  $\begin{pmatrix} 2 \\ 2 \end{pmatrix}$  LEED pattern has not reached maximum intensity. They follow the same dispersion as the saturated layer indicating the overlayer at  $\theta = 0.55$  is islands of the same structure.

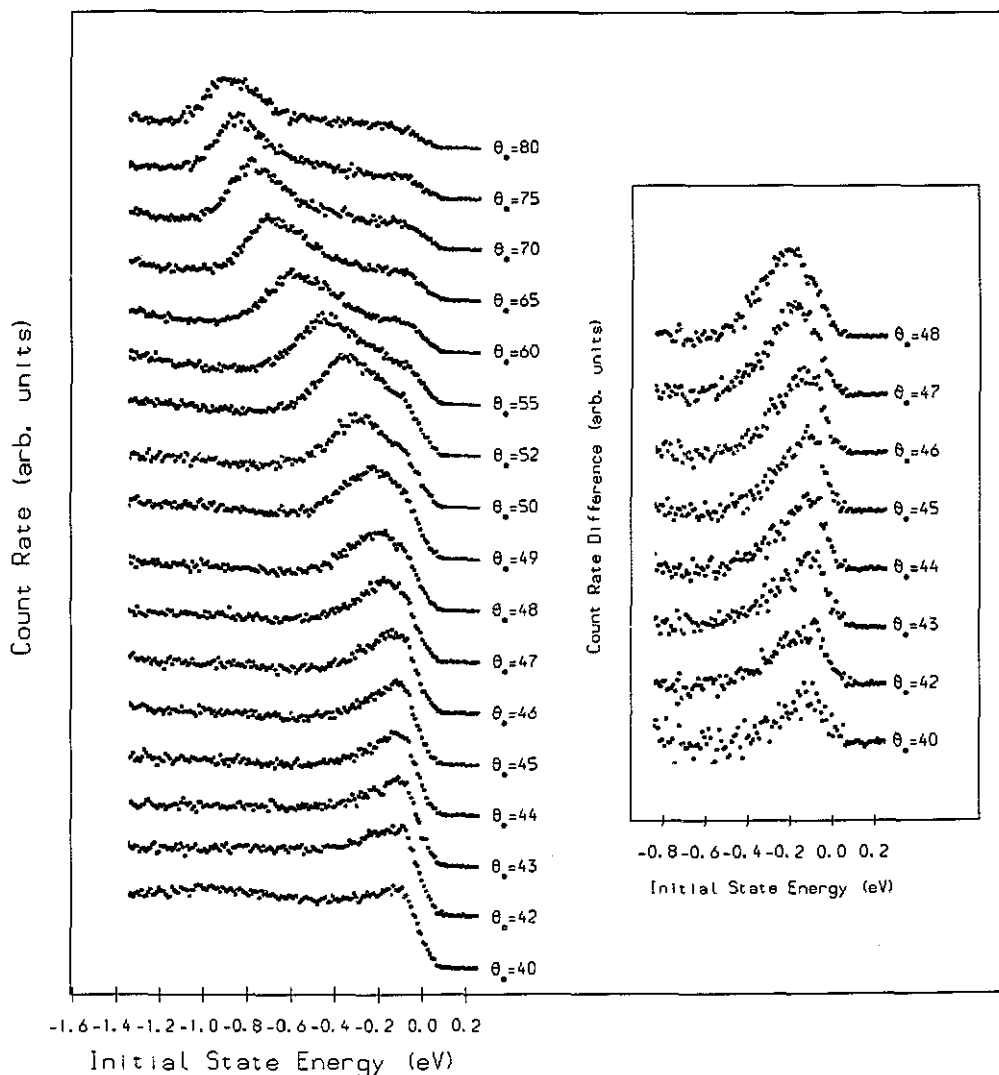


Figure 3. Photoelectron spectra at  $h\nu = 7.87$  eV from the  $(\frac{22}{21})$  Tl overlayer at a coverage,  $\theta = 0.6$  and a temperature of 100 K, as a function of electron emission angle,  $\theta_e$ , showing the dispersion of the Tl 6p feature. The inset shows spectra around the Fermi level crossing after subtraction of the featureless  $\theta_e = 40^\circ$  spectrum from the  $(\frac{66}{22})$  layer.

The behaviour of the 6p band very close to the Fermi level is difficult to determine. The finite energy resolution of the experiment results in a minimum initial state energy,  $E_i^{\min}$ , below which dispersion is unobservable and plotting the  $E$ - $k$  curve shows the band apparently flatten. In the case of the  $(\frac{22}{22})$  structure  $E_i^{\min} = 95$  meV. Thus bandgaps less than 190 meV (assuming the Fermi level is mid-gap) cannot be measured. Their existence, however, can be detected by observing the rate of decay of the intensity of the 6p feature as it approaches the Fermi level. This is discussed in section 3.3.

Figure 5 shows photoemission spectra from the  $(\frac{66}{22})$  structure for  $\theta_e \geq 40^\circ$  at 100 K. The results are similar to those in figure 3; again the 6p band is seen crossing the Fermi

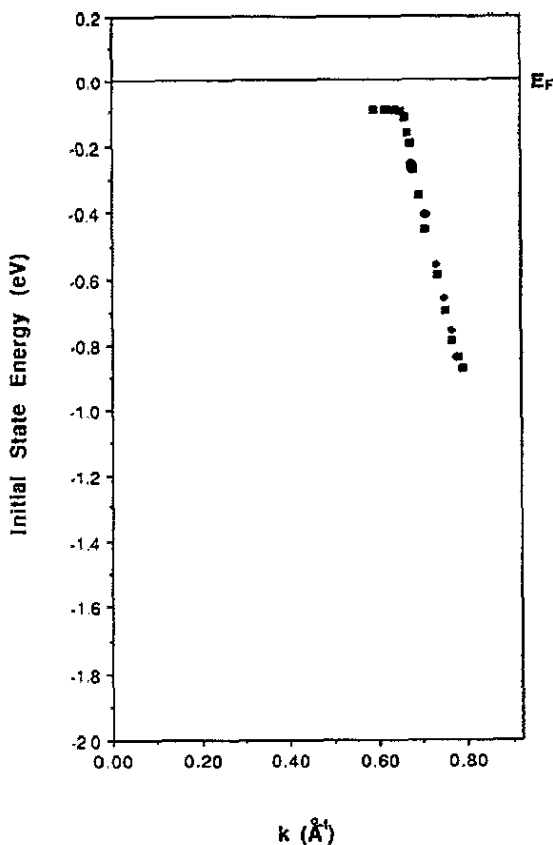


Figure 4.  $E$ - $k$  dispersion of the TI 6p band of the  $\begin{pmatrix} 6 \\ 2 \end{pmatrix}$  TI overlayer at 100 K at coverages  $\theta = 0.55$  ( $\blacklozenge$ ) and  $\theta = 0.6$  ( $\square$ ). The right-hand edge of the figure is the Brillouin zone boundary.

level and dispersing to lower energies. The corresponding  $E$ - $k$  diagram is shown in figure 6. In this case the observed flattening of the band occurs at the slightly higher value of  $E_i = 125$  meV.

On warming the  $\begin{pmatrix} 6 \\ 2 \end{pmatrix}$  structure to 300 K the overlayer LEED spots fade and disappear leaving the  $p(1 \times 1)$  substrate pattern. This indicates that two-dimensional order is lost in the overlayer but whether this is due to a loss of order between neighbouring chains or a complete breakdown of the chain structure has till now been unclear. The photoemission data from the room temperature structure (figure 7) is similar to that for the low-temperature structure with a well defined 6p feature indicating that the chain structure is still intact. An ordering in 1D only as implied here should produce half-order streaks in the LEED pattern rather than a disappearance of the overlayer reflections but the LEED and photoemission results are not inconsistent if account is taken of their differing sampling ranges. We believe the absence of streaks in the LEED pattern is due to short range order on a distance scale sufficient to avoid disruption of the features observed in photoemission ( $>10$  Å) but insufficient to show features in a LEED measurement whose correlation width is of the order 50–100 Å. The 6p band dispersion is plotted in figure 6 and is similar to that at low temperature. The behaviour very close to the Fermi level is different, however, with a value of  $E_i^{\text{min}} \approx 95$  meV. We refer to this overlayer as the room temperature  $\begin{pmatrix} 6 \\ 2 \end{pmatrix}$  structure even though a  $p(1 \times 1)$  pattern is actually observed.

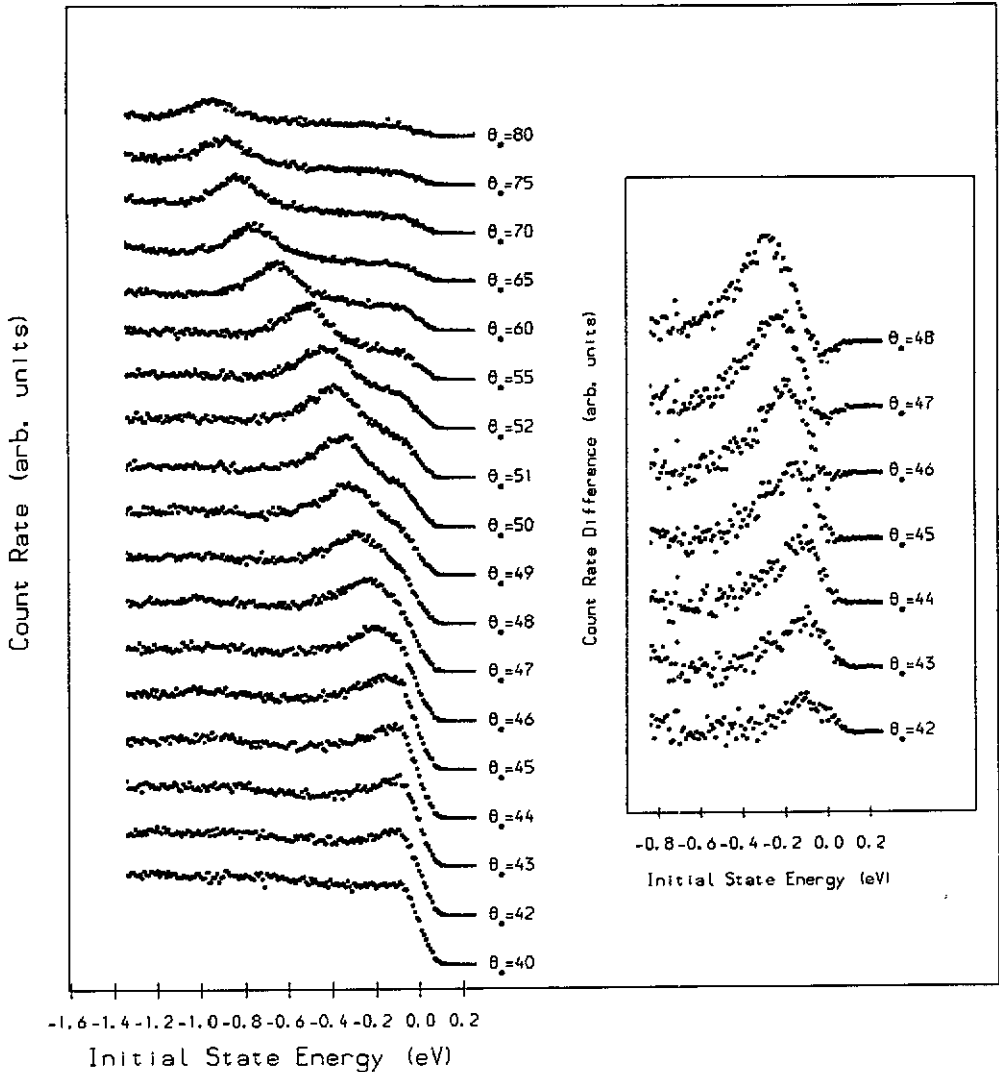


Figure 5. Photoelectron spectra at  $h\nu = 7.87$  eV from the ( $^{66}_{22}$ ) Tl overlayer at a coverage,  $\theta = 0.67$  and a temperature of 100 K, as a function of electron emission angle,  $\theta_e$ , showing the dispersion of the TI 6p feature. The inset shows spectra around the Fermi level crossing after subtraction of the featureless  $\theta_e = 40^\circ$  spectrum.

### 3.3. Behaviour of the 6p band close to the Fermi level

It is important to determine for each overlayer structure whether a Fermi level bandgap exists and if possible to measure its size. This requires the subtraction of a suitable background from photoemission spectra taken at angles corresponding to the Fermi level crossing of the 6p feature. The featureless spectrum at  $\theta_e = 40^\circ$  from the cooled ( $^{66}_{22}$ ) structure (figure 5) has been used as a background for all spectra taken in the range  $40^\circ \leq \theta_e \leq 48^\circ$  after normalization at  $E_i = 0.8$  eV, that is well away from the thallium 6p feature and the copper 3d bands. The background subtracted spectra around the Fermi



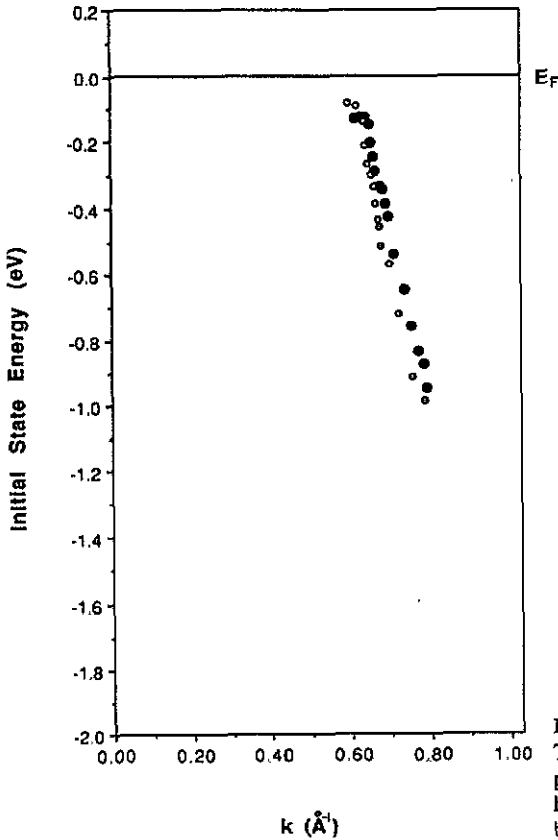


Figure 6.  $E$ - $k$  dispersions of the Tl 6p band of the Tl overlayers at a coverage,  $\theta = 0.67$  at temperatures of 100 K (●) and 300 K (○). The right-hand edge of the figure is the Brillouin zone boundary.

level crossing are shown in the insets in figures 3, 5 and 7. Figure 8 shows the 6p band dispersion and the intensity (area) of the 6p features versus  $k$  in a region within  $0.05 \text{ \AA}^{-1}$  of the Fermi level crossing. The shaded area indicates the portion in which dispersion is unobservable due to the experimental energy resolution. The 6p band from the  $\begin{pmatrix} 2 \\ 2 \\ 2 \end{pmatrix}$  and room temperature  $\begin{pmatrix} 6 \\ 2 \\ 2 \end{pmatrix}$  layers reaches the edge of this region and flattens showing that if there is a gap it is smaller than about 200 meV. The 6p band from the low-temperature  $\begin{pmatrix} 6 \\ 2 \\ 2 \end{pmatrix}$  structure however, flattens off at 125 meV, significantly below the others, indicating the existence of a gap whose width, assuming it is centred around the Fermi level, is 250 meV.

Further evidence of the existence of a bandgap comes from the decay in intensity of the 6p feature. This is seen to be much more rapid in the case of the low-temperature  $\begin{pmatrix} 6 \\ 2 \\ 2 \end{pmatrix}$  structure than that of the  $\begin{pmatrix} 2 \\ 2 \\ 2 \end{pmatrix}$  layer. A band which stops short of the Fermi level will be observed to disappear over a smaller range of  $k$  than one which crosses the Fermi level. The rate of decay of the 6p feature from the room temperature  $\begin{pmatrix} 6 \\ 2 \\ 2 \end{pmatrix}$  structure is intermediate between the other two indicating the existence of a gap whose width is below the 200 meV measurable threshold. The Peierls gap is predicted to be temperature dependent showing a BCS type behaviour so this observation is further evidence that the  $\begin{pmatrix} 6 \\ 2 \\ 2 \end{pmatrix}$  overlayer is dominated by 1D behaviour. The data from the  $\begin{pmatrix} 2 \\ 2 \\ 2 \end{pmatrix}$  layer doesn't rule out the possibility of a very small bandgap but since this would contradict the LEED results which show no evidence for a superstructure, we reject it.

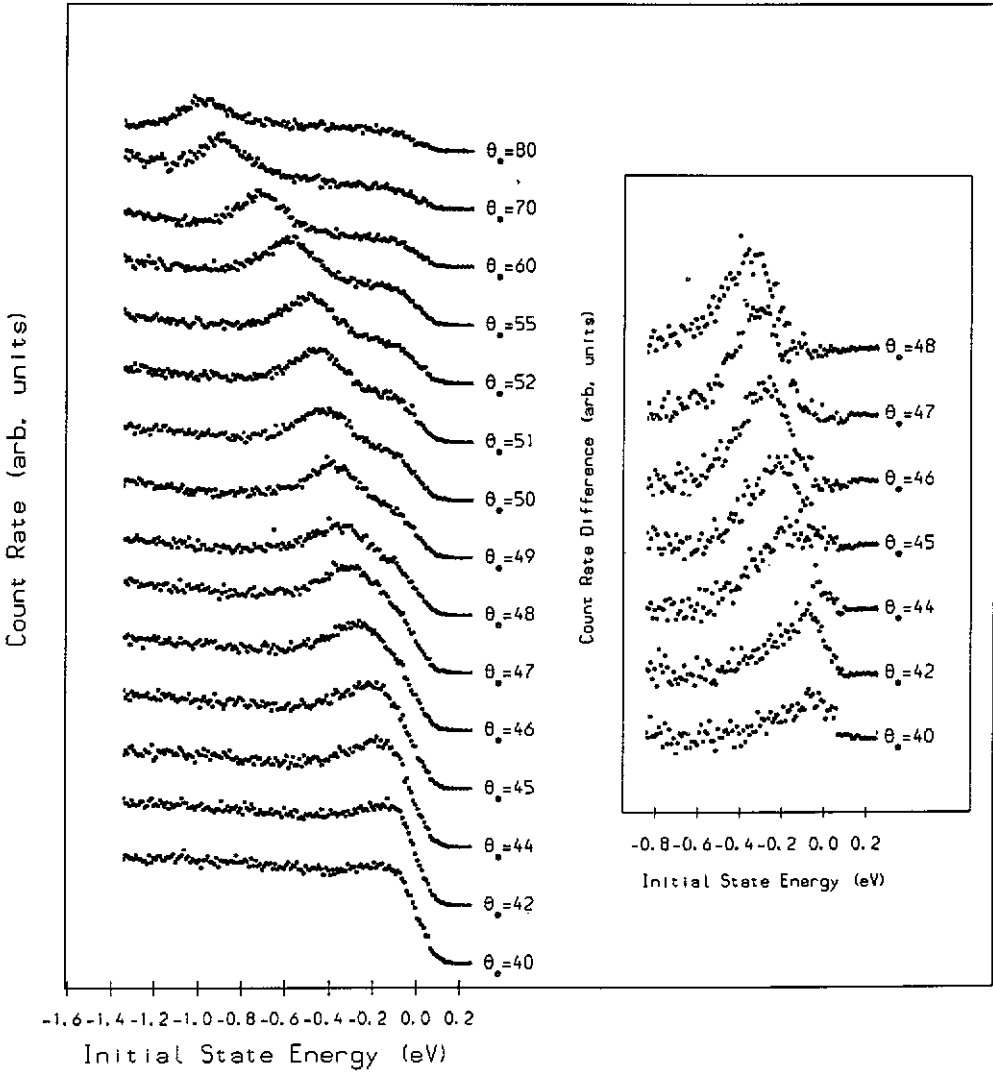


Figure 7. Photoelectron spectra at  $h\nu = 7.87$  eV from the Tl overlayer at a coverage,  $\theta = 0.67$  and a temperature of 300 K, as a function of electron emission angle,  $\theta_e$ , showing the dispersion of the Tl 6p feature. The inset shows spectra around the Fermi level crossing after subtraction of the same background as in figures 3 and 5.

For the low-temperature ( $\begin{smallmatrix} 66 \\ 22 \end{smallmatrix}$ ) structure the gap is at  $k = 0.635 \pm 0.02 \text{ \AA}^{-1}$  while previous work using radiation of 21.2 eV photon energy (Binns *et al* 1984) measured the position of the gap in the second zone to be at  $k = 1.36 \pm 0.05 \text{ \AA}^{-1}$ . This locates the zone boundary at  $k = 1.00 \pm 0.05 \text{ \AA}^{-1}$ , giving an average atomic spacing along the chain,  $3.14 \pm 0.2 \text{ \AA}$ . The observed LEED pattern requires the atomic spacing to be an integer divisor of 12 copper atom spacings, that is,  $30.72 \text{ \AA}$ . We see that 10 thallium atoms, with an average spacing  $3.07 \text{ \AA}$  is the only feasible number. So we conclude that the basis of the ( $\begin{smallmatrix} 66 \\ 22 \end{smallmatrix}$ ) structure contains 10 thallium atoms with an average spacing of  $3.07 \text{ \AA}$  and a 10:12 registry with the substrate atomic spacing. In fact, if the thallium atoms were in

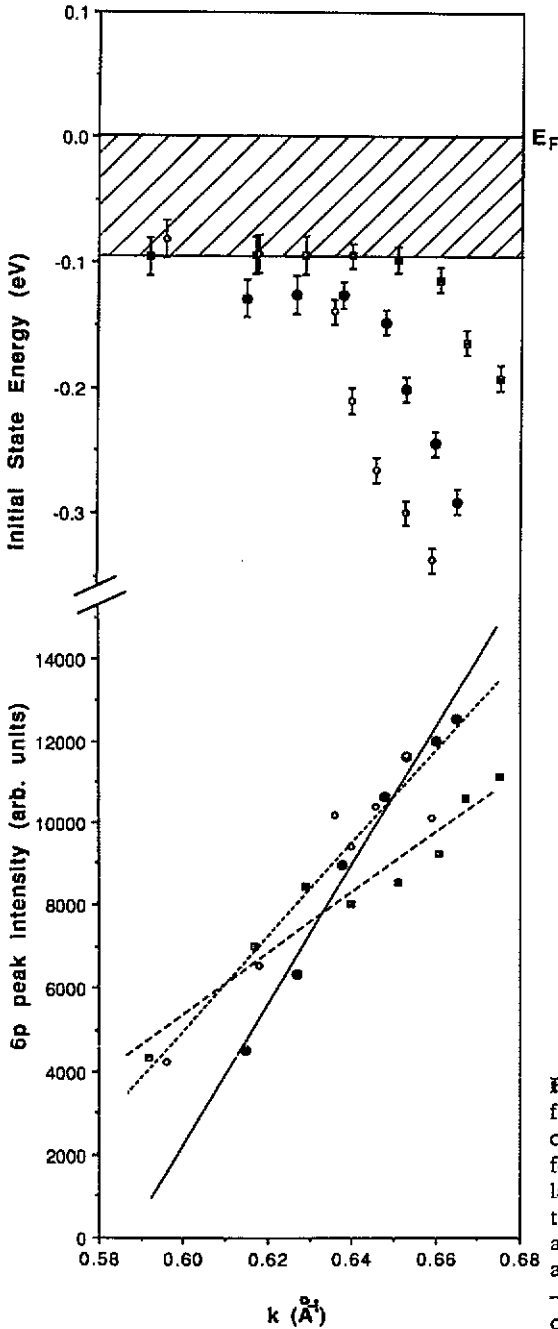


Figure 8. Top half:  $E$ - $k$  dispersion of Tl 6p bands from various overlayers in detail within  $0.05 \text{ \AA}^{-1}$  of the Fermi level crossing. The symbols are as follows:  $\square$ ,  $\left(\frac{2 \times 2}{2 \times 2}\right)$  overlayer at 100 K;  $\bullet$ ,  $\left(\frac{6 \times 6}{2 \times 2}\right)$  overlayer at 100 K;  $\circ$ ,  $\left(\frac{6 \times 6}{2 \times 2}\right)$  overlayers at 300 K. Bottom half: intensity of the Tl 6p feature versus  $k$  around the Fermi level crossing. The symbols are as follows:  $-\square-$ ,  $\left(\frac{2 \times 2}{2 \times 2}\right)$  overlayer at 100 K;  $-\bullet-$ ,  $\left(\frac{6 \times 6}{2 \times 2}\right)$  overlayers at 100 K;  $-\circ-$ ,  $\left(\frac{6 \times 6}{2 \times 2}\right)$  overlayer at 300 K.

the positions predicted by the average spacing, registry with the substrate would occur every 6 copper atoms and a different LEED pattern would be observed. It is the existence of the superstructure which loses this lower registry. In this case a simple dimerization would give the  $\left(\frac{6 \times 6}{2 \times 2}\right)$  LEED pattern. The structure is shown schematically in figure 1(b).

In summary we find that at low temperature (100 K) the  $\begin{pmatrix} 66 \\ 22 \end{pmatrix}$  layer is composed of TI chains which have undergone a Peierls distortion consisting of a dimerization with a corresponding Fermi level bandgap of width 250 meV. On heating this layer to room temperature the chains remain intact and the continued existence of a bandgap, whose width is reduced to below the measurable threshold of 200 meV, indicates the persistence of a superstructure. The observed loss of LEED pattern is thus due to a random phase of the CDW in going from chain to chain. The slightly lower density and more commensurate  $\begin{pmatrix} 22 \\ 22 \end{pmatrix}$  structure shows no evidence for a Fermi level bandgap in agreement with the LEED data which indicates an undistorted chain.

#### 4. Discussion

In all studies of pseudo-1D systems it is important to consider three-dimensional interactions, that is to quantify the anisotropy. This can be characterized by the ratio of electron bandwidths parallel and perpendicular to the chains,  $\gamma$ . We can define a critical value,  $\gamma_{\min}$ , such that for  $\gamma > \gamma_{\min}$ , the system is three-dimensional, albeit highly anisotropic, but for  $\gamma < \gamma_{\min}$ , the system is essentially one-dimensional in nature. In this region, the behaviour is dominated by collective effects and fluctuations and the processes involved in electrical transport are fundamentally altered. The value of  $\gamma_{\min}$  is system dependent and not well defined since different aspects of 1D behaviour will emerge at different values of  $\gamma$  but following Firsov *et al* (1985) we take, as a working hypothesis,  $\gamma_{\min} < 10\%$ .

One of the main observations in this report is the onset of a Peierls distortion in going from the  $\begin{pmatrix} 22 \\ 22 \end{pmatrix}$  structure at  $\theta = 0.6$  to the  $\begin{pmatrix} 66 \\ 22 \end{pmatrix}$  structure at  $\theta = 0.67$ . The inter-chain distance is the same at both coverages, that is 5.12 Å, but the latter structure has a higher atomic density along the chain. Heine (1967) predicted an inverse fifth power law connecting the electron bandwidth with the atomic separation so we estimate  $\gamma = 13\%$  for the chains at  $\theta = 0.6$  and  $\gamma = 8\%$  for the higher-density chains. Thus the difference in behaviour between the two structures may be attributed to the value of  $\gamma$  falling below  $\gamma_{\min}$ . This evaluation assumes an isotropic interaction between thallium atoms which is clearly not the case. Directional bonding will tend to reduce the above estimates for  $\gamma$ .

Another possible explanation for the difference in behaviour is the interaction with the substrate. Thallium chains on Ag(100) (Binns *et al* 1986) do not undergo a Peierls distortion yet, by a similar analysis their anisotropy corresponds to  $\gamma = 3\%$ . In this case the suppression of 1D behaviour was attributed to the interfacial energy term between overlayer and substrate. It is possible for thallium to have a 1:1 registry with the substrate thus maximizing this term. In the case of thallium on Cu(100) the  $\begin{pmatrix} 22 \\ 22 \end{pmatrix}$  layer at  $\theta = 0.6$  has a 3:4 registry with the substrate but the higher density structure would, in the absence of a superstructure, have a 5:6 registry. It is possible that the higher registry at the lower coverage results in a sufficiently large interfacial energy to inhibit the formation of a CDW.

The  $\begin{pmatrix} 66 \\ 22 \end{pmatrix}$  structure becomes disordered as the sample temperature is increased from 100 to 300 K. In the absence of LEED spot intensity measurements we cannot specify a transition temperature, only that the overlayer pattern is completely absent above about 220 K. The photoemission results indicated that the thallium chains are intact and that the superstructure is still present at room temperature so the disorder is mainly due to a random phase of the CDW in going from chain to chain. Mean field theory predicts

that the Peierls gap follows a BCS type temperature dependence and the transition temperature,  $T_c^{mf}$ , is given by (Rice 1975):

$$k_B T_c^{mf} = E_g/3.52$$

where  $E_g$  is the energy gap at  $T = 0$ . For an energy gap of 250 meV, this corresponds to 820 K. The neglect of fluctuations inherent in the mean field approach, however, results in a gross overestimation of the transition temperature. In fact a perfect 1D system ( $\gamma = 0$ ) has no long-range order except at  $T = 0$ . It is the interaction between chains in a pseudo-1D system which produces a phase transition at a finite temperature between  $T = 0$  and  $T = T_c^{mf}$  and in the case of thallium chains on Cu(100), it appears that the transition temperature is higher than 300 K.

## 5. Conclusion

Two thallium chain structures adsorbed on Cu(100) have been investigated using angle-resolved photoelectron spectroscopy. The lower density structure shows no evidence for the formation of a CDW. This is due either to a high commensurability between overlayer and substrate or an insufficiently high anisotropy. With increased coverage there is a reduction in the atomic spacing along the chains which gives a greater anisotropy and a lower commensurability with the substrate. This system has a detectable Fermi level gap, estimated to be 250 meV, and has thus undergone a Peierls distortion which is probably a dimerization along the chains. At about 220 K, the phase of the superstructure is random perpendicular to the chains and two-dimensional order is lost. The distortion along individual chains, however, persists at room temperature.

## Acknowledgment

This work was supported by SERC grant number GR/E/60680.

## References

- Binns C, Barthés-Labrousse M-G and Norris C 1984 *J. Phys. C: Solid State Phys.* **17** 1465  
 Binns C, Newstead D A, Norris C, Barthés-Labrousse M-G and Stephenson P C 1986 *J. Phys. C: Solid State Phys.* **19** 829  
 Binns C and Norris C 1982 *Surf. Sci.* **115** 395  
 Firsov Yu A, Prigodin V N and Seidel Chr 1985 *Phys. Rep.* **126** 245  
 Heine V 1967 *Phys. Rev.* **153** 673  
 Lieb E H and Mattis D C 1966 *Mathematical Physics in One-Dimension* (New York: Academic)  
 Peierls R E 1964 *Quantum Theory of Solids* (Oxford: Clarendon)  
 Rice M J 1975 *Low-Dimensional Co-operative Phenomena* ed H J Keller (New York: Plenum)  
 Schultz T D 1979 *The Physics and Chemistry of Low-Dimensional Solids* ed L Alcàser (Dordrecht: Reidel)  
 Solyom J 1979 *Adv. Phys.* **28** 201